

## Glassy Dynamics in Geometrically Frustrated Coulomb Liquids without Disorder

Samiyeh Mahmoudian,<sup>1</sup> Louk Rademaker,<sup>2</sup> Arnaud Ralko,<sup>3</sup> Simone Fratini,<sup>3</sup> and Vladimir Dobrosavljević<sup>1</sup>

<sup>1</sup>*Department of Physics and National High Magnetic Field Laboratory, Florida State University, Tallahassee, Florida 32306, USA*

<sup>2</sup>*Kavli Institute for Theoretical Physics, University of California Santa Barbara, Santa Barbara, California 93106, USA*

<sup>3</sup>*Institut Néel-CNRS and Université Joseph Fourier, Boîte Postale 166, F-38042 Grenoble Cedex 9, France*

(Received 13 January 2015; published 8 July 2015)

We show that introducing long-range Coulomb interactions immediately lifts the massive ground state degeneracy induced by geometric frustration for electrons on quarter-filled triangular lattices in the classical limit. Important consequences include the stabilization of a stripe-ordered crystalline (global) ground state, but also the emergence of very many low-lying metastable states with amorphous “stripe-glass” spatial structures. Melting of the stripe order thus leads to a frustrated Coulomb liquid at intermediate temperatures, showing remarkably slow (viscous) dynamics, with very long relaxation times growing in Arrhenius fashion upon cooling, as typical of strong glass formers. On shorter time scales, the system falls out of equilibrium and displays the aging phenomena characteristic of supercooled liquids above the glass transition. Our results show remarkable similarity with the recent observations of charge-glass behavior in ultraclean triangular organic materials of the  $\theta$ -(BEDT-TTF)<sub>2</sub> family.

DOI: 10.1103/PhysRevLett.115.025701

PACS numbers: 64.70.Q-, 71.10.-w, 73.20.Qt, 75.25.Dk

Metastability, slow relaxation, and other features of glassy dynamics are often observed in electronic systems at the brink of the metal-insulator transition [1]. These effects, however, are typically attributed to disorder caused by impurities or defects, rather than being an intrinsic feature of strongly interacting electrons. Indeed, “Coulomb glass” behavior [2,3] is well established in disordered insulators [4,5]; in other cases metastability can be caused by disorder-dominated phase separation in the presence of competing orders [6].

A more intriguing possibility was proposed in the heyday of cuprate superconductivity, with the idea of “Coulomb-frustrated phase separation” in lightly doped Mott insulators [7,8]. It suggested the possibility of spontaneous (disorder-unrelated) formation of many complicated patterns of charge density, such as bubbles and stripe crystals [9], or even stripe glasses [10]. Unfortunately, no conclusive theoretical or experimental evidence emerged to support the existence of such phase separation, which long remained more of a theorist’s dream than an accepted mechanism for metastability in electronic systems.

Glassy freezing without disorder, on the other hand, is well established in several systems with geometric frustration, most notably the supercooled liquids [11]. A natural question thus emerges: Can sufficient geometric frustration cause disorder-free glassy behavior of electrons, in (many) situations where phase separation effects are not relevant? Geometric frustration arises, for example, in spin systems on triangular lattices [12,13], sometimes leading to exotic phases like spin liquids [14]; related frustration-driven phenomena in the charge sector have been little explored so far.

A class of systems where one can directly investigate these important questions is represented by the organic triangular compounds of the family  $\theta$ -(BEDT-TTF)<sub>2</sub>MM'(SCN)<sub>4</sub> (in short  $\theta$  – MM') where  $M = \text{Tl, Rb, Cs}$  and  $M' = \text{Co, Zn}$ , which exhibits a notable degree of charge frustration [15]. These materials are quarter-filled; i.e., they have one particle per two lattice sites, and in most cases they display a first order structural transition upon cooling, leading to a charge-ordered insulating ground state. Such a structural transition, however, can be avoided by sufficiently rapid cooling, and the system is found to remain a poor conductor [16], displaying characteristic kinetic slowing down [15,17,18] reminiscent of glassy dynamics. Remarkably, single crystals of these compounds have no significant amount of disorder, as shown by the observation of clear quantum Shubnikov–de Haas oscillations [19], suggesting a possibility of self-generated (disorder-free) glassy behavior of electrons [15].

Despite these significant experimental advances, the following questions remain: (1) What is the dominant physical mechanism that may produce such glassy dynamics of electrons? (2) What is the role of geometric frustration and the range of electron-electron interactions? In this Letter we present a model calculation that provides a clear and physically transparent answer to these important questions. We show that the long-range nature of the Coulomb repulsion plays a crucial role in lifting the massive ground-state degeneracy produced by geometric frustration. However, it does so very weakly, producing an extensive manifold of low-lying metastable states, causing slow relaxation and glassy dynamics up to temperatures above the stripe melting transition, even in the absence of disorder.

*Model.*—We study a system of spinless electrons on a triangular lattice with intersite repulsion  $V_{ij}$ ,

$$H = -t \sum_{\langle i,j \rangle} c_i^\dagger c_j + \frac{1}{2} \sum_{ij} V_{ij} \left( n_i - \frac{1}{2} \right) \left( n_j - \frac{1}{2} \right), \quad (1)$$

where  $t$  is the hopping integral between two neighboring sites and  $c_i^\dagger$  is the electron creation operator. We fix the density to one particle per two sites,  $n = 1/2$ , as appropriate to the  $\theta - MM'$  salts. We also allow for deviations from the perfect triangular lattice, by defining an anisotropy parameter  $\lambda$  via the unit vectors  $a = \hat{y}$  and  $b = \frac{1}{2}(\sqrt{3}\lambda\hat{x} + \hat{y})$  ( $\lambda = 1.16$  for  $\theta$ -CsZn and  $\lambda = 1.26$  for  $\theta$ -RbZn [20]). In what follows we shall consider a maximally frustrated isotropic lattice ( $\lambda = 1$ ) unless otherwise specified.

Charge ordering in organic conductors is customarily attributed to the presence of strong nearest neighbor repulsion, of the form  $V_{ij} = V\delta_{|R_i - R_j|=1}$  [21]. In this case the ground state of Eq. (1) is massively degenerate in the classical limit  $t = 0$ , as any state where each particle has exactly two nearest neighbor sites occupied has an energy per site of  $\epsilon = -V/4$ . Such ordered states include the linear (vertical) and zigzag (horizontal) stripes depicted in Figs. 1(a) and 1(b), as well as any other striped configurations such as the long zigzag stripes of Fig. 1(c).

Interestingly, another class of configurations with exactly the same potential energy can be constructed by dividing the lattice into three sublattices, one of which is filled (“pins”), one empty, and the third is randomly occupied by the remaining particles (“balls”). Figure 1(d) shows one particular example in this class, where the balls, shown as light disks, are themselves ordered. When quantum effects are turned on, the latter can delocalize as Bloch waves on the honeycomb lattice not occupied by the localized pins, leading to a unique ground state whose energy is lower than the stripes, which is termed “pinball liquid” [22]. This occurs because the delocalization of balls in the pinball state yields a kinetic energy gain  $\propto t$ , as opposed to stripes, where only local fluctuations  $\propto t^2/V$  are allowed. For nearest neighbor interactions, quantum fluctuations therefore immediately lift the classical degeneracy, as soon as  $t \neq 0$ .

Real electrons, however, interact through long-range Coulomb interactions. The central observation of this Letter is the fact that the inclusion of an even modest long-range component completely changes the behavior, and dominates over the quantum effects described above at least in the strong coupling regime ( $V/t \gg 1$ ). To make this point, we consider a family of intersite interactions of the form

$$V_{ij} = (1-x)V\delta_{|R_i - R_j|=1} + x \frac{V}{|R_i - R_j|} \quad (2)$$

with  $x \leq 0 \leq 1$ . It reduces to the nearest neighbor interaction for  $x = 0$ , and to the full long range Coulomb potential for  $x = 1$ .

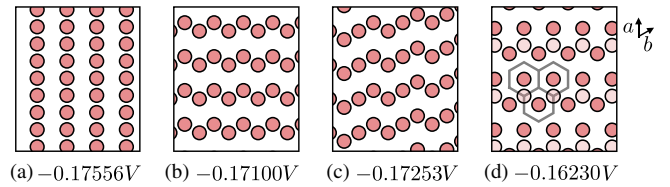


FIG. 1 (color online). Periodic charge configurations on the triangular lattice with  $n = 1/2$  particles per site: (a) linear stripes, (b) short zigzag stripes, (c) long zigzag stripes, and (d) the lowest energy three-sublattice structure (see text), with the corresponding energies calculated for the long range Coulomb potential [ $x = 1$  in Eq. (2)]. For nearest-neighbor interactions only ( $x = 0$ ), all these states are degenerate in energy,  $\epsilon = -V/4$ .

*Stripe order and metastability.*—The energies of different charge configurations in the presence of the interaction Eq. (2) can be evaluated using standard Ewald summation techniques [23]. We find that the crucial effect of adding a long-range component is the lifting of the ground-state degeneracy already at the classical level, with the linear stripes of Fig. 1(a) having a lower energy than any other configuration as soon as  $x > 0$ . The numerical results for the full Coulomb potential ( $x = 1$ ) are reported in Fig. 1 for a set of relevant examples.

First, the resulting finite (albeit small) electrostatic energy gap,  $\gtrsim 0.01$  V, separating three-sublattice configurations [Fig. 1(d)] from the stripes [Fig. 1(a)] implies that stripe order must survive as the ground state even in the presence of quantum fluctuations, within a *finite* interval of  $t$  in which the quantum processes associated with the pinball phase can be neglected. We confirmed this result by performing exact diagonalization (ED) calculations on finite-size clusters of up to 16 sites, using again Ewald potentials to account for the long range tail of the interaction. Our ED results show that for the full Coulomb potential ( $x = 1$ ) a first order transition from stripes to pinball occurs at  $(t/V)_c \approx 0.05$ . The stability of stripes is further enhanced with increasing anisotropy [22], resulting in a critical  $(t/V)_c$  which rapidly increases with  $\lambda$  (the critical value is  $(t/V)_c \approx 0.08$  already at  $\lambda = 1.16$ ). Both the rigorous stability argument given above (for infinitesimal  $t$ ) and our ED results (for finite  $t$ ) therefore indicate that the behavior obtained from a classical model, where stripes are the lowest energy state, should be at least qualitatively valid to describe systems with a small ratio  $t/V$ . This regime is actually relevant to the organic salts under study, where *ab initio* calculations suggest typical values  $t/V \sim 0.05$ – $0.1$  [24,25]. Moreover, mean-free paths are so small in organic solids that the electron motion can be considered as classical to a good approximation [26]. We shall therefore consider in what follows the  $t = 0$  limit of Eq. (1).

Second, the manifold of states that were degenerate in the short range model now gives rise to a macroscopic number of quasidegenerate configurations, that are spread within typically 0.01 V from the ground state. Evaluating

the strength  $V = e^2/\epsilon a$  of the Coulomb potential, with typical values  $\epsilon \approx 3$  for the dielectric constant and  $a \sim 5 \text{ \AA}$  for the lattice constant, yields  $V \sim 1 \text{ eV}$  and  $0.01 \text{ V} \approx 100 \text{ K}$ . This estimate shows that these configurations are within the thermally accessible range, so that they should participate in the classical fluctuations of the electronic system.

The reason behind such a low energy scale is that energy differences only depend on the interaction between distant neighbors (as pointed out above, nearest neighbor interaction terms are the same by construction for all the configurations in the manifold); the longer the length scale  $|R_i - R_j|$ , the more the considered charge configurations will look uniform, and the interaction energy will eventually average out to very comparable values. The barriers between these states are, however, much larger. They are actually of order  $V$ , because going from one configuration to the other necessarily involves local rearrangements of the charge. As we proceed to show, such a large *local* energy scale, contrasted to the much smaller *global* energy scale corresponding to long-range rearrangements, causes the system to get easily “stuck” in one of these states, which therefore become metastable.

*Glassy behavior.*—To illustrate the dynamic slowing down in the correlated liquid above the freezing transition, reflecting the emergence of many metastable states, we examine our system at finite temperature through classical Monte Carlo simulations. We use the METROPOLIS algorithm with local (nearest neighbor) updates [3] to mimic real-time dynamics of hopping electrons, since in the organic materials the electrons have exponentially suppressed beyond-nearest neighbor hopping. The long-range nature of the interaction is taken into account using Ewald summation [23], with lattice sizes  $L = 12, 24, 36$ , and  $48$ . Note that  $L = 48$  corresponds to  $L^2/2 = 1152$  electrons.

Starting from zero temperature with the linear stripe ordered phase, we find that for the pristine Coulomb potential ( $x = 1$ ), the stripe order remains stable up to the temperature  $T_c \sim 0.038 \text{ V}$ , where the system undergoes a first-order transition to an (isotropic) fluid phase with significant short-range order. A detailed characterization of the first-order stripe-melting transition is beyond the scope of this work. We shall here focus our full attention to understanding the structure and the dynamics of the correlated fluid phase above the melting transition.

A typical fluid configuration is shown in Fig. 2(c), where we observe finite-size striped domains with random orientations (linear stripes are sixfold degenerate, corresponding to three orientations and two sublattice origins). To quantify the observed short-range order, we computed the structure factor within the correlated fluid phase, defined as the thermally averaged density-density correlation function  $S(\mathbf{k}) = \langle n_{\mathbf{k}} n_{-\mathbf{k}} \rangle$ . Typical results obtained at  $T = 0.04 \text{ V}$ , just above the melting transition, are displayed in Fig. 2. For these results, we equilibrated 1000 independent simulations,

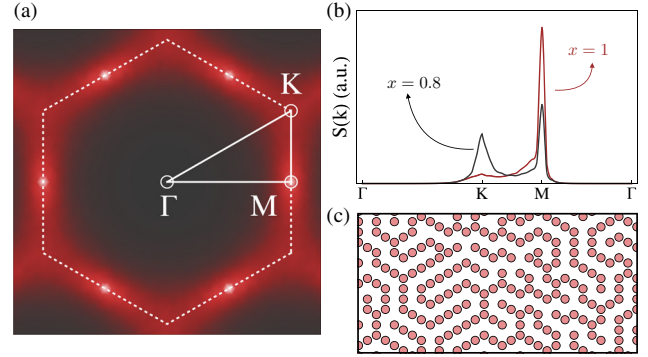


FIG. 2 (color online). (a) Structure factor  $C(k)$  of the frustrated Coulomb liquid obtained for a  $L = 36$  lattice size and averaged over 1000 independent equilibrated Monte Carlo runs at  $T = 0.04 \text{ V}$  above the melting transition. Clearly defined diffuse Bragg peaks are observed at the (linear) stripe order wave vector  $M = [(2\pi/\sqrt{3}), 0]$  and symmetry equivalent points. (b) Same, plotted along the high-symmetry lines of the Brillouin zone drawn in panel (a) (arb. units). (c) A snapshot illustrating a typical “stripe liquid” configuration.

with 50 000 measurement sweeps per simulation. A sharp peak is found at the  $M$  points, signalling the existence of local stripe order, corresponding to the linear stripes of Fig. 2(a). Remarkably, this peak coexists with a broader feature at the  $K$  points, reminiscent of the classical three sublattice configurations which are precursor to the pinball liquid phase. Note that the relative weight of these two features is directly controlled by the long range strength  $x$ , as shown in Fig. 2(b). A diffuse background is also visible along the whole Brillouin zone edge, indicative of a correlation hole around each electron. The coexistence of two competing ordering wave vectors and the emergence of diffuse lines in the structure factor is a distinctive feature of  $\theta - MM'$  salts that is naturally captured when long range interactions are included.

To further characterize the role of striped correlations in the fluid phase, we turn our attention to the dynamics and set out to describe the dynamic relaxation processes, closely following the approaches previously used to investigate (disordered) Coulomb glasses [3]. Our runs were  $5 \times 10^5$  Monte Carlo sweeps long, where one sweep constitutes  $L^2$  update attempts. Physical quantities were monitored as a function of time (measured in number of sweeps) for each sample and the results were averaged over between 500 and 1000 initial random configurations.

We computed the local autocorrelation function

$$C(t + t_w, t_w) = \frac{2}{N} \sum_i \langle \delta n_i(t + t_w) \delta n_i(t_w) \rangle, \quad (3)$$

where  $t_w$  is the waiting time measured in Monte Carlo sweeps. Following Ref. [3], we first quickly “quench” (cool down) the system from a random initial configuration to the desired temperature  $T$ , and then allow the system to relax

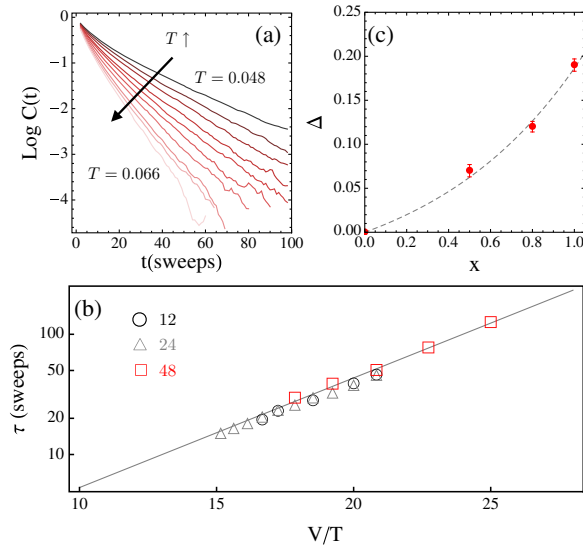


FIG. 3 (color online). (a) The local autocorrelation function  $C(t)$  of the stripe liquid obtained via Monte Carlo simulations on lattices of sizes  $L = 12, 24, 48$  at different temperatures, showing exponential decay at long times (time in units of the elementary MC step). (b) For all studied sizes, the decay time  $\tau$  follows a clear Arrhenius scaling  $\tau \sim e^{\Delta/T}$  in the studied interval, signalling strong glassy behavior. (c) The activation energy  $\Delta$  as a function of the strength  $x$  of the long range interaction tail.

for a waiting time  $t = t_w$ , before collecting data for the autocorrelation function. We perform such studies at each temperature for several values of  $t_w$ ; the system is equilibrated when  $t_w$  is sufficiently long so that the autocorrelation function becomes independent of the waiting time,  $C(t + t_w, t_w) = C(t)$ . The long-time exponential tail of  $C(t)$  [Fig. 3(a)] then directly gives us the desired relaxation time  $\tau(T)$ , which we generally find to be comparable to the required time to equilibrate the system. The relaxation time thus found displays Arrhenius behavior [11],

$$\tau(T) = \tau_0 e^{\Delta/T} \quad (4)$$

as illustrated in Fig. 3(b) for  $x = 1$ . The strong (that is, Arrhenius instead of the “fragile” Vogel-Tammann-Fulcher) glass behavior obtained here is reminiscent of the precursor of the cluster glass phase in  $\theta$ -CsZn, as shown by the resistivity aging and noise experiments performed in Ref. [18], where it was found that  $\Delta \approx 2600$  K. Setting  $V \sim 1$  eV, the activation energy  $\Delta \approx 0.2$  V found in the simulations for  $x = 1$  [Fig. 3(c)] corresponds to 2300 K. A hopping time  $\tau_0 \approx 10^{-11}$ – $10^{-10}$  s can be estimated from the measured dc conductivity at high temperatures by assuming classical incoherent transport. The resulting  $\tau(T)$  from Eq. (4) is also in good agreement with the experimental values [18], providing quantitative support to the present theoretical picture.

The dramatic slowing down arising in this correlated stripe liquid directly reflects the long-range nature of the

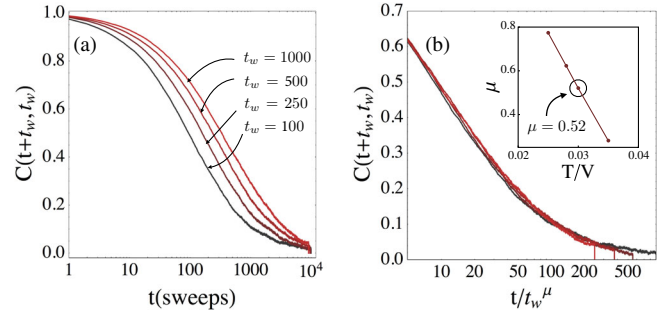


FIG. 4 (color online). (a) Autocorrelation function for different waiting times, at  $T = 0.03$ . Equilibrium is restored only if the waiting time  $t_w$  is sufficiently long; the corresponding relaxation time  $\tau \approx 10^3$ , and for  $t_w < \tau$ , the system displays history dependence and aging, as typically found in glass formers in the supercooled liquid regime. (b) Data can be collapsed in terms of  $t/t_w^\mu$ , with  $\mu$  a temperature dependent aging exponent (inset), similarly as in (disordered) Coulomb glasses [3].

Coulomb interaction. To illustrate this point, we gradually decrease the amplitude  $x$  of the long-range Coulomb potential. We find that the same qualitative behavior is found for any nonzero value of  $x$ , and the relaxation time still displays simple activated behavior, however, with an  $x$ -dependent activation energy, which is seen to decrease as  $x$  is reduced, and vanish at  $x = 0$  [Fig. 3(c)] [27].

The results presented above correspond to an equilibrated fluid state at temperatures above the crystal melting temperature  $T_c$ . Experimental results for  $\theta$ - $MM'$  compounds indeed show that the dynamical slowing down and the short-range charge correlations are already manifest above the melting temperature, as a precursor for further glassy freezing in the supercooled regime [15,18]. At temperatures below the stripe melting transition, the relaxation time becomes very long, which allows a study of the dynamics for waiting times shorter than  $t_w < \tau(T)$ . In this regime the autocorrelation function depends on both  $t$  and the waiting time  $t_w$ , displaying characteristic “aging” behavior [3]. Here, the autocorrelation function  $C(t + t_w, t_w)$  assumes a scaling form  $F(t/t_w^\mu)$  where  $\mu$  is the aging exponent, as illustrated in Fig. 4. We found such aging behavior in the entire supercooled regime  $T < T_c$ , demonstrating dynamical behavior precisely of the form expected for supercooled liquids around the glass transition, consistent with results obtained for Coulomb glasses [3]. In fact, our qualitative and even quantitative results are very similar to this well-known glass former, indicating that robust glassy behavior emerges in our model even in the absence of disorder.

*Outlook.*—We have shown that the interplay of long range interactions and geometric frustration plays a singular role in Coulomb liquids, producing a multitude of metastable states, slow relaxation, and most characteristic features of disorder-free glassy dynamics in the correlated liquid regime, as recently observed in the two-dimensional organic conductors

$\theta - MM'$ . The general mechanism identified here, however, may be expected to be significant in a much broader class of systems, including many families of complex (e.g., spinel) oxides with not only triangular, but also kagome and pyrochlore lattices. Quantum fluctuations [28] can be conveniently tuned in these systems, for example by applying pressure or appropriate chemical doping. The resulting quantum critical behavior of such self-generated Coulomb glasses thus arises as one of the most attractive avenues of experimental and theoretical investigation in future work, not only from the perspective of basic science research, but also as an important issue for the next generation of electronic devices [29].

The authors thank K. Kanoda, T. Sato, F. Kagawa, L. Balents, Z. Nussinov, and J. Zaanen for interesting discussions. L. R. was supported by the Dutch Science Foundation (NWO) through a Rubicon grant. This work is supported by the French National Research Agency through Grant No. ANR-12-JS04-0003-01 SUBRISSYME. Work in Florida (S. M. and V. D.) was supported by the NSF Grants No. DMR-1005751 and No. DMR-1410132. V. D. would like to thank CPTGA for financing a visit to Grenoble, and KITP at UCSB, where part of the work was performed.

- 
- [1] V. Dobrosavljević, N. Trivedi, and J.M. Valles Jr, *Conductor Insulator Quantum Phase Transitions* (Oxford University Press, Oxford, 2012).
- [2] A. A. Pastor and V. Dobrosavljević, *Phys. Rev. Lett.* **83**, 4642 (1999).
- [3] A. B. Kolton, D. R. Grempel, and D. Dominguez, *Phys. Rev. B* **71**, 024206 (2005).
- [4] A. Vaknin, Z. Ovadyahu, and M. Pollak, *Phys. Rev. Lett.* **84**, 3402 (2000).
- [5] S. Bogdanovich and D. Popović, *Phys. Rev. Lett.* **88**, 236401 (2002).
- [6] E. Dagotto, *Science* **309**, 257 (2005).
- [7] L. P. Gor'kov and A. V. Sokol, *JETP Lett.* **46**, 333 (1987).
- [8] V. J. Emery and S. A. Kivelson, *Physica (Amsterdam)* **209C**, 597 (1993).
- [9] R. Jamei, S. Kivelson, and B. Spivak, *Phys. Rev. Lett.* **94**, 056805 (2005).
- [10] J. Schmalian and P. G. Wolynes, *Phys. Rev. Lett.* **85**, 836 (2000).
- [11] P. G. Debenedetti and F. H. Stillinger, *Nature (London)* **410**, 259 (2001).
- [12] L. Balents, *Nature (London)* **464**, 199 (2010).
- [13] A. P. Ramirez, *Annu. Rev. Mater. Sci.* **24**, 453 (1994).
- [14] Y. Shimizu, K. Miyagawa, K. Kanoda, M. Maesato, and G. Saito, *Phys. Rev. Lett.* **91**, 107001 (2003).
- [15] F. Kagawa, T. Sato, K. Miyagawa, K. Kanoda, Y. Tokura, K. Kobayashi, R. Kumai, and Y. Murakami, *Nat. Phys.* **9**, 419 (2013).
- [16] K. Hashimoto, S. C. Zhan, R. Kobayashi, S. Iguchi, N. Yoneyama, T. Moriwaki, Y. Ikemoto, and T. Sasaki, *Phys. Rev. B* **89**, 085107 (2014).
- [17] F. Nad, P. Monceau, and H. M. Yamamoto, *Phys. Rev. B* **76**, 205101 (2007).
- [18] T. Sato, F. Kagawa, K. Kobayashi, K. Miyagawa, K. Kanoda, R. Kumai, Y. Murakami, and Y. Tokura, *Phys. Rev. B* **89**, 121102 (2014).
- [19] S. Klepper, G. Athas, J. Brooks, M. Tokumoto, T. Kinoshita, N. Tamura, and M. Kinoshita, *Synth. Met.* **70**, 835 (1995).
- [20] H. Mori, S. Tanaka, and T. Mori, *Phys. Rev. B* **57**, 12023 (1998).
- [21] H. Seo, J. Merino, H. Yoshioka, and M. Ogata, *J. Phys. Soc. Jpn.* **75**, 051009 (2006).
- [22] C. Hotta and N. Furukawa, *Phys. Rev. B* **74**, 193107 (2006).
- [23] A. Y. Toukmaji and J. A. Board Jr, *Comput. Phys. Commun.* **95**, 73 (1996).
- [24] K. Nakamura, Y. Yoshimoto, T. Kosugi, R. Arita, and M. Imada, *J. Phys. Soc. Jpn.* **78**, 083710 (2009).
- [25] L. Cano-Cortés, A. Dölfen, J. Merino, J. Behler, B. Delley, K. Reuter, and E. Koch, *Eur. Phys. J. B* **56**, 173 (2007).
- [26] S. Fratini, D. Mayou, and S. Ciuchi, arXiv:1505.02686.
- [27] T. Mori, *J. Phys. Soc. Jpn.* **72**, 1469 (2003).
- [28] T. E. Markland, J. A. Morrone, B. J. Berne, K. Miyazaki, E. Rabani, and D. R. Reichman, *Nat. Phys.* **7**, 134 (2011).
- [29] H. Oike, F. Kagawa, N. Ogawa, A. Ueda, H. Mori, M. Kawasaki, and Y. Tokura, *Phys. Rev. B* **91**, 041101 (2015).